

## BUCKLING OF IMPERFECT SANDWICH CYLINDERS UNDER AXIAL COMPRESSION

R. C. TENNYSON and K. C. CHAN

University of Toronto, Institute for Aerospace Studies, Toronto, Ontario, Canada M3H 5T6

**Abstract**—An analytical study has been carried out to determine the effect of axisymmetric shape imperfections on the compressive buckling strength of sandwich cylinders having isotropic facings and orthotropic, shear deformable cores. Buckling solutions are presented as a function of imperfection amplitude, wavelength and the core shear flexibility coefficients. Non-shear deformable cores have also been considered and results compared to isotropic cylinders based on an “equivalent” thickness parameter.

### INTRODUCTION

Circular cylindrical shell structures are widely used in aerospace vehicles, such as rockets, satellite components and aircraft fuselage sections. Although these structures are commonly fabricated from metals, advanced composites are also gaining widespread usage because of their higher strength/weight and stiffness/weight ratios. Prior to the advent of composites, however, the development of sandwich construction emerged because of the significant stiffness/weight improvements offered (Plantema, 1966). Most of the buckling analyses performed on sandwich cylinders have considered isotropic (Leggett and Hopkins, 1949; Teichmann *et al.*, 1951; Stein and Meyers, 1952; Wang *et al.*, 1955; Almroth, 1964; Barteld and Mayers, 1967) and orthotropic facings (March and Kuenzi, 1957; Reese and Bert, 1969, 1974; Zahn and Kuenza, 1963) with one recent report dealing with composite skins (Cheung and Tennyson, 1988). In all of these models, the core is regarded as “shear deformable” and the cylinders are treated as geometrically “perfect” in shape.

Up to this point in time, no Koiter-type imperfection analysis has been carried out on circular cylindrical sandwich cylinders under axial compression, to assess the extent to which these structures are sensitive to geometric shape imperfections. This report presents approximate analytical solutions for the buckling stress of axisymmetric imperfect sandwich cylinders with isotropic facings as a function of imperfection amplitude, wavelength and core shear stiffness. An “equivalent thickness” parameter is also defined that allows the design engineer to estimate “knock-down” factors for sandwich cylinders based on isotropic cylinder results, including the effect of random shape imperfections (Tennyson *et al.*, 1971).

### FORMULATION OF PROBLEM

#### Shell configuration

The axisymmetric imperfect sandwich cylinder geometry and coordinate system are shown in Fig. 1. The cylinder geometry is characterized by its length  $L$ , radius of the median

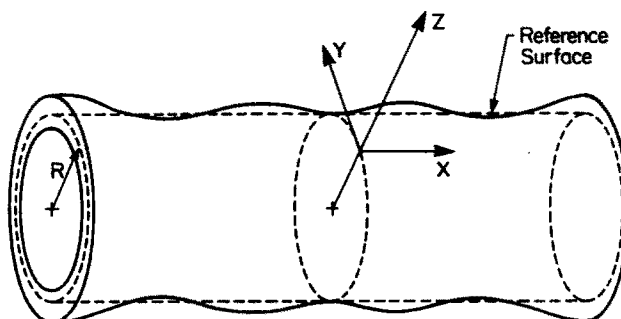


Fig. 1. Circular cylindrical shell with axisymmetric shape imperfections.

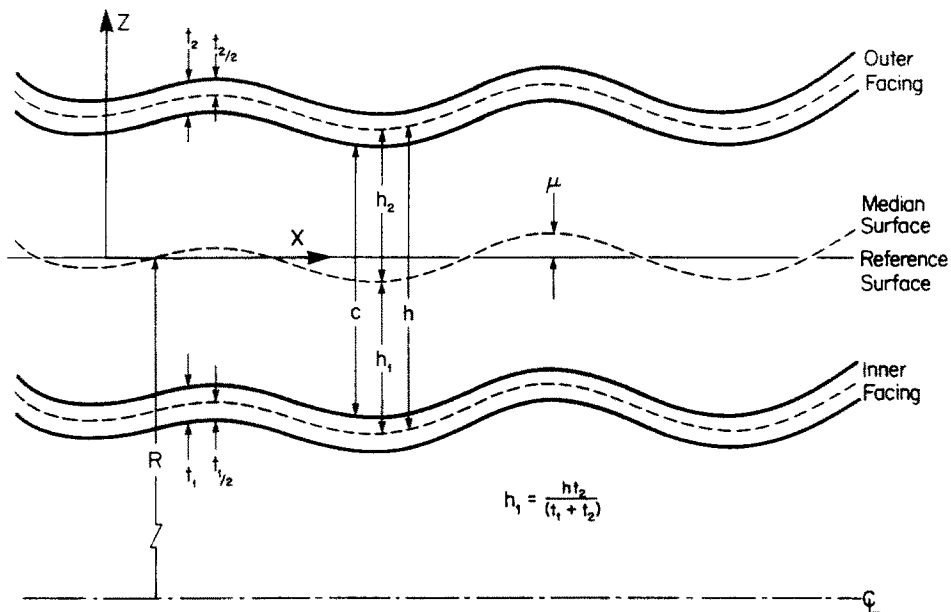


Fig. 2. Geometrical definition of sandwich shell wall.

surface  $R$ , inner face thickness  $t_1$ , outer face thickness  $t_2$ , core thickness  $c$  and imperfection amplitude  $\mu$  (see Fig. 2).

Let the reference surface be the median surface of the geometrically perfect cylinder, as defined by:

$$h_1 = \frac{ht_2}{t_1 + t_2}. \quad (1)$$

Thus the separation between the mid-surfaces of the inner and outer facings is

$$h = c + \frac{t_1 + t_2}{2}. \quad (2)$$

The coordinate system,  $x, y, z$  is measured with respect to the reference surface in the axial, circumferential and radial directions, respectively. The components of displacement  $u, v$  and  $w$  of a point on the perfect shell are the displacements in the  $x, y$  and  $z$  directions.

#### Restrictions and assumptions

The following restrictions apply to the analytical model:

- (1) Both facings are made of the same isotropic material.
- (2) The core is orthotropic with one axis of orthotropy parallel to the axis of the cylinder.
- (3) The core and facings have uniform elastic properties.
- (4) Facings and core are of constant thickness throughout the shell wall. The two facings may have different thicknesses.
- (5) There are no initial wrinkles in the facings, i.e. the separation between the facings is constant.
- (6) There is no failure of bonding between facings and core.
- (7) Facings are sufficiently thin (compared to the core) to be treated as membranes, i.e. the facings have in-plane stiffness but no flexural stiffness about their mid-surfaces.
- (8) The shell thickness is small compared with the radius of curvature  $R$ .
- (9) The cylinder is sufficiently long to ignore end boundary conditions.
- (10) There is no intercell buckling.

The following assumptions are made in the analysis :

- (1) Displacements  $u, v,$  and  $w$  are small compared with the plate thickness.
- (2) Strains  $\epsilon_x, \epsilon_y$  and  $\gamma_{xy}$  are small compared to unity (small strain theory).
- (3) The core carries no in-plane stress.
- (4) Normal stiffness of the core is infinite so that instability associated with wrinkling of facings and other normal strain effects is not included. In practice, sandwich cylinders with honeycomb core will not fail by wrinkling of facings when there is no failure of bonding between facings and core.
- (5) The transverse normal stress is negligible, i.e.  $\sigma_z = 0$ .

EQUILIBRIUM AND COMPATIBILITY EQUATIONS

*Strain–displacement relations*

Using the nonlinear Karman–Donnell strain–displacement relations, unit strains at a point in the shell can be expressed as,

$$\begin{aligned} \epsilon_x &= \frac{\partial \bar{u}}{\partial x} + \frac{1}{2} \left( \frac{\partial \bar{w}}{\partial x} \right)^2, & \epsilon_y &= \frac{\partial \bar{v}}{\partial y} + \frac{\bar{w}}{R} + \frac{1}{2} \left( \frac{\partial \bar{w}}{\partial y} \right)^2, & \epsilon_z &= 0 \\ \gamma_{xy} &= \frac{\partial \bar{v}}{\partial x} + \frac{\partial \bar{u}}{\partial y} + \frac{\partial \bar{w}}{\partial x} \frac{\partial \bar{w}}{\partial y}, & \gamma_{yz} &= \frac{\partial \bar{w}}{\partial y} + \frac{\partial \bar{v}}{\partial z}, & \gamma_{xz} &= \frac{\partial \bar{u}}{\partial z} + \frac{\partial \bar{w}}{\partial x}. \end{aligned} \tag{3}$$

The condition of zero normal strain is the result of the assumption that the transverse normal stiffness is infinite. This also implies that  $\bar{w}$  is not a function of  $z$ . For thin shells,  $\bar{u}$  and  $\bar{v}$  may be assumed to vary linearly in the  $z$  direction. The relations between the displacement components  $u, v$  and  $w$  of the deformed median surface and the displacement components  $\bar{u}, \bar{v}$  and  $\bar{w}$  of a point in the shell are :

$$\bar{u} = u - z\beta_x, \quad \bar{v} = v - z\beta_y, \quad \bar{w} = w, \tag{4}$$

where  $\beta_x$  and  $\beta_y$  can be interpreted physically as the components of change of slope of the normal to the undeformed median surface.

When the thickness of the facings is sufficiently small compared with the core, and when the transverse core shear strain is small, the strains for the mid-surfaces of the facings can be approximated by the strains at the facing and core interface. In this assumption, the facings are effectively considered to be membranes.

Thus by substituting eqn (4) into eqn (3) the strain–displacement relations become,

$$\epsilon_x = \epsilon_x^0 - z \frac{\partial \beta_x}{\partial x}, \quad \epsilon_y = \epsilon_y^0 - z \frac{\partial \beta_y}{\partial y}, \quad \gamma_{xy} = \gamma_{xy}^0 - z \left( \frac{\partial \beta_y}{\partial x} + \frac{\partial \beta_x}{\partial y} \right), \quad \gamma_{yz} = \gamma_{yz}^0, \quad \gamma_{xz} = \gamma_{xz}^0, \tag{5}$$

where the median surface strains  $\epsilon_x^0, \epsilon_y^0, \gamma_{xy}^0, \gamma_{yz}^0$  and  $\gamma_{xz}^0$  are given by :

$$\begin{aligned} \epsilon_x^0 &= \frac{\partial u}{\partial x} + \frac{1}{2} \left( \frac{\partial w}{\partial x} \right)^2, & \epsilon_y^0 &= \frac{\partial v}{\partial y} + \frac{w}{R} + \frac{1}{2} \left( \frac{\partial w}{\partial y} \right)^2, \\ \gamma_{xy}^0 &= \frac{\partial v}{\partial x} + \frac{\partial u}{\partial y} + \frac{\partial w}{\partial x} \frac{\partial w}{\partial y}, & \gamma_{yz}^0 &= \frac{\partial w}{\partial y} - \beta_y, & \gamma_{xz}^0 &= \frac{\partial w}{\partial x} - \beta_x \end{aligned} \tag{6}$$

assuming the median surface displacements  $u, v$  do not vary in the  $z$  direction. The initial stress-free lateral deviation  $w$  of the median surface is assumed to be small, but finite values are also permissible provided that :

$$|w_0| \ll R \quad \text{and} \quad \left| \frac{\partial w_0}{\partial x} \right| \ll 1. \quad (7)$$

Shallow shell theory requires that the radius of curvature of the shape imperfection cannot be excessively small as expressed by;

$$R \left| \frac{\partial^2 w_0}{\partial x^2} \right| \leq 0(1). \quad (8)$$

The modified strain–displacement relations for the median surface including the initial deviation term  $w_0$  are:

$$\begin{aligned} \varepsilon_x^0 &= \frac{\partial u}{\partial x} + \frac{1}{2} \left( \frac{\partial w}{\partial x} \right)^2 + \frac{\partial w}{\partial x} \frac{\partial w_0}{\partial x}, & \varepsilon_y^0 &= \frac{\partial v}{\partial y} + \frac{w}{R} + \frac{1}{2} \left( \frac{\partial w}{\partial y} \right)^2 + \frac{\partial w}{\partial y} \frac{\partial w_0}{\partial y}, \\ \gamma_{xy}^0 &= \frac{\partial v}{\partial x} + \frac{\partial u}{\partial y} + \frac{\partial w}{\partial x} \frac{\partial w}{\partial y} + \frac{\partial w_0}{\partial x} \frac{\partial w}{\partial y} + \frac{\partial w}{\partial x} \frac{\partial w_0}{\partial y}, \\ \gamma_{yz}^0 &= \frac{\partial w}{\partial y} - \beta_y, & \gamma_{xz}^0 &= \frac{\partial w}{\partial x} - \beta_x. \end{aligned} \quad (9)$$

#### STRESS-STRAIN RELATIONS

##### Facings

The in-plane stress–strain relations for the isotropic facings in a plane stress state are:

$$\sigma_x = \frac{E_f}{(1-\nu^2)} (\varepsilon_x + \nu \varepsilon_y), \quad \sigma_y = \frac{E_f}{(1-\nu^2)} (\varepsilon_y + \nu \varepsilon_x), \quad \tau_{xy} = \frac{E_f}{2(1+\nu)} \gamma_{xy} \quad (10)$$

where  $E_f$  = modulus of elasticity of facings.

Stress–strain relations in terms of  $\beta_x$ ,  $\beta_y$  and the median surface strains  $\varepsilon_x^0$ ,  $\varepsilon_y^0$  and  $\gamma_{xy}^0$  can be obtained by substituting eqn (5) into eqn (10):

$$\begin{aligned} \sigma_x &= \frac{E_f}{(1-\nu^2)} \left[ \varepsilon_x^0 + \nu \varepsilon_y^0 - z \left( \frac{\partial \beta_x}{\partial x} + \nu \frac{\partial \beta_y}{\partial y} \right) \right] \\ \sigma_y &= \frac{E_f}{(1-\nu^2)} \left[ \varepsilon_y^0 + \nu \varepsilon_x^0 - z \left( \frac{\partial \beta_y}{\partial y} + \nu \frac{\partial \beta_x}{\partial x} \right) \right] \\ \tau_{xy} &= \frac{E_f}{(1-\nu^2)} \left[ \gamma_{xy}^0 - z \left( \frac{\partial \beta_y}{\partial x} + \frac{\partial \beta_x}{\partial y} \right) \right]. \end{aligned} \quad (11)$$

##### Core

Assuming the core resists only transverse shear and does not carry any in-plane stresses, then the stress–strain relations for the core are:

$$\tau_{xz} = G_x \gamma_{xz} = G_x \gamma_{xz}^0, \quad \tau_{yz} = G_y \gamma_{yz} = G_y \gamma_{yz}^0, \quad \sigma_x = \sigma_y = \tau_{xy} = 0. \quad (12)$$

##### Shell forces and moments

An equivalent system of force and moment resultants is considered to be acting at the median surface of an element of the shell, as given by the following definitions:

Stress resultants :

$$\begin{bmatrix} N_x \\ N_y \\ N_{xy} \end{bmatrix} = \int_{-h_1-t_1/2}^{h_2+t_2/2} \begin{bmatrix} \sigma_x \\ \sigma_y \\ \tau_{xy} \end{bmatrix} dz. \tag{13}$$

Transverse shear stress resultants :

$$\begin{bmatrix} Q_x \\ Q_y \end{bmatrix} = \int_{-h_1-t_1/2}^{h_2+t_2/2} \begin{bmatrix} \tau_{xz} \\ \tau_{yz} \end{bmatrix} dz. \tag{14}$$

Moment resultants :

$$\begin{bmatrix} M_x \\ M_y \\ M_{xy} \end{bmatrix} = \int_{-h_1-t_1/2}^{h_2+t_2/2} \begin{bmatrix} \sigma_x \\ \sigma_y \\ \tau_{xy} \end{bmatrix} z dz \tag{15}$$

where the integration is taken across the whole shell wall and  $h_1, h_2$  are the distances of the middle surfaces of the inner and outer facings, respectively, from the median surface of the total shell wall as depicted in Fig. 2.

After performing the integration in eqn (13), using the expressions for the in-plane stresses  $\sigma_x, \sigma_y$  and  $\tau_{xy}$  from eqn (11), the in-plane stress resultants in terms of  $\beta_x, \beta_y$  and the median surface strains are :

$$\begin{aligned} N_x &= \frac{E_f}{(1-\nu^2)} \left[ (t_1+t_2)(\epsilon_x^0 + \nu\epsilon_y^0) - (h_2t_2 - h_1t_1) \left( \frac{\partial\beta_x}{\partial x} + \nu \frac{\partial\beta_y}{\partial y} \right) \right] \\ N_y &= \frac{E_f}{(1-\nu^2)} \left[ (t_1+t_2)(\epsilon_y^0 + \nu\epsilon_x^0) - (h_2t_2 - h_1t_1) \left( \frac{\partial\beta_y}{\partial x} + \nu \frac{\partial\beta_x}{\partial y} \right) \right] \\ N_{xy} &= \frac{E_f}{(1-\nu^2)} \left[ \gamma_{xy}^0 - (h_2t_2 - h_1t_1) \left( \frac{\partial\beta_y}{\partial x} - \frac{\partial\beta_x}{\partial y} \right) \right]. \end{aligned} \tag{16}$$

The transverse shear stresses  $\tau_{yz}$  and  $\tau_{xz}$  in the facings are equal to the transverse shear stresses in the core at the facings, and vanish on the free surfaces. Assuming a linear variation of transverse shear stresses across the facings and using eqn (12) for the transverse shear stresses in the core, the transverse shear stress resultants, after integration of eqn (14), become :

$$Q_x = G_x h \gamma_{xz}^0 = G_x h \left( \frac{\partial w}{\partial x} - \beta_x \right), \quad Q_y = G_y h \gamma_{yz}^0 = G_y h \left( \frac{\partial w}{\partial y} - \beta_y \right). \tag{17}$$

Again, using expressions for in-plane stresses from eqn (11), the moment resultants, after integration of eqn (15), become :

$$\begin{aligned} M_x &= \frac{E_f}{(1-\nu^2)} \left[ (h_2t_2 - h_1t_1)(\epsilon_x^0 + \nu\epsilon_y^0) - \left( h_2^2t_2 + \frac{t_2^3}{12} + h_1^2t_1 + \frac{t_1^3}{12} \right) \left( \frac{\partial\beta_x}{\partial x} + \nu \frac{\partial\beta_y}{\partial y} \right) \right] \\ M_y &= \frac{E_f}{(1-\nu^2)} \left[ (h_2t_2 - h_1t_1)(\epsilon_y^0 + \nu\epsilon_x^0) - \left( h_2^2t_2 + \frac{t_2^3}{12} + h_1^2t_1 + \frac{t_1^3}{12} \right) \left( \frac{\partial\beta_y}{\partial x} + \nu \frac{\partial\beta_x}{\partial y} \right) \right] \\ M_{xy} &= \frac{E_f}{(1-\nu^2)} \left[ (h_2t_2 - h_1t_1)\gamma_{xy}^0 - \left( h_2^2t_2 + \frac{t_2^3}{12} + h_1^2t_1 + \frac{t_1^3}{12} \right) \left( \frac{\partial\beta_y}{\partial x} - \frac{\partial\beta_x}{\partial y} \right) \right]. \end{aligned} \tag{18}$$

With the definition of the median surface given by eqn (1), the coupling between in-plane strains and the rotation of the normal disappears, and the stress and moment resultants simplify to:

$$N_x = \frac{A}{(1-\nu^2)} (\epsilon_x^0 + \nu \epsilon_y^0), \quad N_y = \frac{A}{(1-\nu^2)} (\epsilon_y^0 + \nu \epsilon_x^0), \quad N_{xy} = \frac{A}{2(1+\nu)} \gamma_{xy}^0 \quad (19)$$

$$M_x = -D \left( \frac{\partial \beta_x}{\partial x} + \nu \frac{\partial \beta_y}{\partial y} \right), \quad M_y = -D \left( \frac{\partial \beta_y}{\partial y} + \nu \frac{\partial \beta_x}{\partial x} \right), \quad M_{xy} = \frac{-D(1-\nu)}{2} \left( \frac{\partial \beta_y}{\partial x} + \frac{\partial \beta_x}{\partial y} \right), \quad (20)$$

where the in-plane stiffness ( $A$ ) and bending stiffness ( $D$ ) parameters are given by:

$$A = E_f(t_1 + t_2) \quad (21)$$

$$D = \frac{E_f}{(1-\nu^2)} \left[ \frac{h^2 t_1 t_2}{t_1 + t_2} + \frac{1}{12} (t_1^3 + t_2^3) \right] \\ \approx \left( \frac{E_f h^2 t_1 t_2}{(1-\nu^2)(t_1 + t_2)} \right) \quad \text{for } t_1, t_2 \ll c. \quad (22)$$

#### Equilibrium equations

When the transverse normal stiffness of the sandwich shell is infinite, the equations of force and moment equilibrium are the same as those for conventional cylindrical shells. For a thin circular cylindrical shell the equilibrium equations are:

Equilibrium of horizontal forces:

$$\frac{\partial N_x}{\partial x} + \frac{\partial N_{xy}}{\partial y} = 0, \quad \frac{\partial N_y}{\partial y} + \frac{\partial N_{xy}}{\partial x} = 0. \quad (23)$$

Equilibrium of vertical forces:

$$\frac{\partial Q_x}{\partial x} + \frac{\partial Q_y}{\partial y} + N_x \left( \frac{\partial^2 w}{\partial x^2} + \frac{\partial^2 w_0}{\partial x^2} \right) + 2N_{xy} \left( \frac{\partial^2 w}{\partial x \partial y} + \frac{\partial^2 w_0}{\partial x \partial y} \right) + N_y \left( \frac{\partial^2 w}{\partial y^2} + \frac{\partial^2 w_0}{\partial y^2} - \frac{1}{R} \right) = 0. \quad (24)$$

Equilibrium of moments:

$$\frac{\partial M_x}{\partial x} + \frac{\partial M_{xy}}{\partial y} = Q_x, \quad \frac{\partial M_{xy}}{\partial x} + \frac{\partial M_y}{\partial y} = Q_y. \quad (25)$$

An Airy stress function is defined such that it will satisfy the equilibrium equations [eqn (23)] identically, i.e.

$$N_x = \frac{\partial^2 F}{\partial y^2}, \quad N_y = \frac{\partial^2 F}{\partial x^2}, \quad N_{xy} = -\frac{\partial^2 F}{\partial x \partial y}. \quad (26)$$

By substituting for  $M_x$ ,  $M_y$  and  $M_{xy}$  from eqn (20) into eqn (25),  $Q_x$  and  $Q_y$  can be expressed in terms of  $\beta_x$  and  $\beta_y$  as:

$$\begin{aligned}
 Q_x &= -D \left[ \frac{\partial^2 \beta_x}{\partial x^2} + \frac{(1+\nu)}{2} \frac{\partial^2 \beta_y}{\partial x \partial y} + \frac{(1-\nu)}{2} \frac{\partial^2 \beta_x}{\partial y^2} \right] \\
 Q_y &= -D \left[ \frac{\partial^2 \beta_y}{\partial y^2} + \frac{(1+\nu)}{2} \frac{\partial^2 \beta_x}{\partial x \partial y} + \frac{(1-\nu)}{2} \frac{\partial^2 \beta_y}{\partial x^2} \right].
 \end{aligned}
 \tag{27}$$

Replacing  $Q_x$  and  $Q_y$  in the above equations by expressions from eqn (17), the relations between  $w$  and  $\beta_x, \beta_y$  are:

$$\begin{aligned}
 \beta_x - \frac{\partial w}{\partial x} &= \frac{D}{G_x h} \left[ \frac{\partial^2 \beta_x}{\partial x^2} + \frac{(1+\nu)}{2} \frac{\partial^2 \beta_y}{\partial x \partial y} + \frac{(1-\nu)}{2} \frac{\partial^2 \beta_x}{\partial y^2} \right] \\
 \beta_y - \frac{\partial w}{\partial y} &= \frac{D}{G_y h} \left[ \frac{\partial^2 \beta_y}{\partial y^2} + \frac{(1+\nu)}{2} \frac{\partial^2 \beta_x}{\partial x \partial y} + \frac{(1-\nu)}{2} \frac{\partial^2 \beta_y}{\partial x^2} \right].
 \end{aligned}
 \tag{28}$$

Substituting for  $Q_x$  and  $Q_y$  from eqn (27) into eqn (24), the equilibrium equation for transverse normal forces becomes:

$$\begin{aligned}
 D \left[ \frac{\partial^3 \beta_x}{\partial x^3} + \frac{\partial^3 \beta_y}{\partial x^2 \partial y} + \frac{\partial^3 \beta_x}{\partial x \partial y^2} + \frac{\partial^3 \beta_y}{\partial y^3} \right] &= \frac{\partial^2 F}{\partial y^2} \left( \frac{\partial^2 w}{\partial x^2} + \frac{\partial^2 w_0}{\partial x^2} \right) - 2 \frac{\partial^2 F}{\partial x \partial y} \left( \frac{\partial^2 w}{\partial x \partial y} + \frac{\partial^2 w_0}{\partial x \partial y} \right) \\
 &\quad + \frac{\partial^2 F}{\partial x^2} \left( \frac{\partial^2 w}{\partial y^2} + \frac{\partial^2 w_0}{\partial y^2} - \frac{1}{R} \right).
 \end{aligned}
 \tag{29}$$

*Compatibility equation*

After eliminating  $u$  and  $v$  from the median surface strain–displacement relations [eqn (9)], an equation for the lateral deflection  $w$  in terms of the median surface strains  $\epsilon_x^0, \epsilon_y^0$  and  $\gamma_{xy}^0$  is obtained:

$$\begin{aligned}
 \frac{\partial^2 \epsilon_x^0}{\partial y^2} + \frac{\partial^2 \epsilon_y^0}{\partial x^2} - \frac{\partial^2 \gamma_{xy}^0}{\partial x \partial y} &= \frac{1}{R} \frac{\partial^2 w}{\partial x^2} + \left( \frac{\partial^2 w}{\partial x \partial y} \right)^2 - \frac{\partial^2 w}{\partial x^2} \frac{\partial^2 w}{\partial y^2} \\
 &\quad - \left( \frac{\partial^2 w_0}{\partial x^2} \frac{\partial^2 w}{\partial y^2} - 2 \frac{\partial^2 w}{\partial x \partial y} \frac{\partial^2 w_0}{\partial x \partial y} + \frac{\partial^2 w}{\partial x^2} \frac{\partial^2 w_0}{\partial y^2} \right).
 \end{aligned}
 \tag{30}$$

The median surface strains can of course be replaced by the stress resultants using the following Hooke’s law relations:

$$\epsilon_x^0 = \frac{1}{A} (N_x - \nu N_y), \quad \epsilon_y^0 = \frac{1}{A} (N_y - \nu N_x), \quad \gamma_{xy}^0 = \frac{2(1+\nu)}{A} N_{xy}.
 \tag{31}$$

Hence one can derive the final form of the compatibility equation in terms of the Airy stress function [see eqn (26)] and the lateral deflection  $w$ :

$$\frac{1}{A} \nabla^4 F = \frac{1}{R} \frac{\partial^2 w}{\partial x^2} + \left( \frac{\partial^2 w}{\partial x \partial y} \right)^2 - \frac{\partial^2 w}{\partial x^2} \frac{\partial^2 w}{\partial y^2} - \left( \frac{\partial^2 w_0}{\partial x^2} \frac{\partial^2 w}{\partial y^2} - 2 \frac{\partial^2 w}{\partial x \partial y} \frac{\partial^2 w_0}{\partial x \partial y} + \frac{\partial^2 w}{\partial x^2} \frac{\partial^2 w_0}{\partial y^2} \right).
 \tag{32}$$

SPECIAL CASES

(a) *Isotropic core* ( $G_x = G_y$ )

When the core is isotropic, the equilibrium equation for transverse normal forces can be expressed in terms of  $w$  and  $F$  only. From eqn (17),

$$\beta_x = \frac{\partial w}{\partial x} - \frac{Q_x}{Gh}, \quad \beta_y = \frac{\partial w}{\partial y} - \frac{Q_y}{Gh}.$$

Substituting for  $\beta_x$  and  $\beta_y$  into the equilibrium equation [eqn (29)] yields,

$$D\nabla^4 w - \frac{D}{Gh} \nabla^2 \left( \frac{\partial Q_x}{\partial x} + \frac{\partial Q_y}{\partial y} \right) = \frac{\partial^2 F}{\partial y^2} \left( \frac{\partial^2 w}{\partial x^2} + \frac{\partial^2 w_0}{\partial x^2} \right) - 2 \frac{\partial^2 F}{\partial x \partial y} \left( \frac{\partial^2 w}{\partial x \partial y} + \frac{\partial^2 w_0}{\partial x \partial y} \right) + \frac{\partial^2 F}{\partial x^2} \left( \frac{\partial^2 w}{\partial y^2} + \frac{\partial^2 w_0}{\partial y^2} - \frac{1}{R} \right). \quad (33)$$

Eliminating the term  $(\partial Q_x/\partial x) + (\partial Q_y/\partial y)$  from eqn (33) and eqn (24) gives:

$$D\nabla^4 w = \left( 1 - \frac{D}{Gh} \nabla^2 \right) \left[ \frac{\partial^2 F}{\partial y^2} \left( \frac{\partial^2 w}{\partial x^2} + \frac{\partial^2 w_0}{\partial x^2} \right) - 2 \frac{\partial^2 F}{\partial x \partial y} \left( \frac{\partial^2 w}{\partial x \partial y} + \frac{\partial^2 w_0}{\partial x \partial y} \right) + \frac{\partial^2 F}{\partial x^2} \left( \frac{\partial^2 w}{\partial y^2} + \frac{\partial^2 w_0}{\partial y^2} - \frac{1}{R} \right) \right]. \quad (34)$$

The above equilibrium equation together with the compatibility equation, eqn (32), are the two governing equations in terms of the two unknowns  $w$  and  $F$  for sandwich cylinders with isotropic cores.

(b) *Non-shear deformable core* ( $G = \infty$ )

The equilibrium equation for sandwich cylinders with a non-shear deformable core can be immediately obtained by setting the core shear modulus  $G$  to infinity, i.e.

$$D\nabla^4 w = \frac{\partial^2 F}{\partial y^2} \left( \frac{\partial^2 w}{\partial x^2} + \frac{\partial^2 w_0}{\partial x^2} \right) - 2 \frac{\partial^2 F}{\partial x \partial y} \left( \frac{\partial^2 w}{\partial x \partial y} + \frac{\partial^2 w_0}{\partial x \partial y} \right) + \frac{\partial^2 F}{\partial x^2} \left( \frac{\partial^2 w}{\partial y^2} + \frac{\partial^2 w_0}{\partial y^2} - \frac{1}{R} \right). \quad (35)$$

The above equation and the compatibility equation, eqn (32), are exactly the same as those for homogeneous isotropic shells except for the stiffness terms  $A$  and  $D$ . Thus all previous analytical results for isotropic cylinders can be immediately applied to sandwich cylinders with non-shear deformable cores when the appropriate in-plane stiffness  $A$  and bending stiffness  $D$  terms are used.

(c) *Isotropic cylinder—no core* ( $c = 0$ )

By setting  $c = 0$ ,

$$A = Et \quad \text{and} \quad D = \frac{Et^3}{12(1-\nu^2)}$$

where  $t = t_1 + t_2$ , and the previous equilibrium and compatibility equations reduce to the isotropic cylinder case.

## BUCKLING ANALYSIS

### *Prebuckling axisymmetric solution*

Assuming an initial axisymmetric shape imperfection, one can write the prebuckling lateral deflection function as



$$w(x, y) = w^*(x)$$

where the asterisk denotes the prebuckling solution.

The solution for the Airy stress function in the prebuckled state is of the following form :

$$F(x, y) = -\frac{1}{2}N_0y^2 + F^*(x) \tag{36}$$

where  $N_0$  is the axially applied load per unit run at the edge.

For the axisymmetric solution,

$$\beta_x(x, y) = \beta_x^*(x) \quad \text{and} \quad \beta_y(x, y) = 0. \tag{37}$$

After substituting these equations into eqns (28), (29) and (32), the four nonlinear governing equations reduce to three linear equations in  $F^*$ ,  $w^*$  and  $\beta_x^*$  for the prebuckling state, i.e.

$$\frac{1}{A} \frac{\partial^4 F^*}{\partial x^4} = \frac{1}{R} \frac{\partial^2 w^*}{\partial x^2}, \quad \beta_x^* - \frac{\partial w^*}{\partial x} = \frac{D}{G_x h} \frac{\partial^2 \beta_x^*}{\partial x^2}, \quad D \frac{\partial^3 \beta_x^*}{\partial x^3} = -N_0 \left( \frac{\partial^2 w^*}{\partial x^2} + \frac{\partial^2 w_0}{\partial x^2} \right) - \frac{1}{R} \frac{\partial^2 F^*}{\partial x^2}. \tag{38}$$

The initial axisymmetric shape imperfection can be written as,

$$w_0(x) = -\mu \cos\left(\frac{2\pi x}{l_x}\right). \tag{39}$$

The order of magnitude of the imperfection amplitude  $\mu$  relative to the imperfection wavelength  $l_x$ , as required by eqn (8), is given by

$$\frac{4\mu\pi^2}{l_x^2} \leq 0(1). \tag{40}$$

From physical considerations, a particular solution is taken to be in the form :

$$F^*(x) = N \cos\left(\frac{2\pi x}{l_x}\right), \quad w^*(x) = K + M \cos\left(\frac{2\pi x}{l_x}\right), \quad \beta_x^*(x) = P \sin\left(\frac{2\pi x}{l_x}\right). \tag{41}$$

Substituting the above assumed solution into three linear differential equations, eqn (38), results in three linear algebraic equations from which  $N$ ,  $M$  and  $P$  can be easily solved, i.e.

$$N = \frac{-\mu\lambda\alpha}{2\rho^2(\lambda_0 - \lambda)}, \quad M = \frac{-\mu\lambda}{(\lambda_0 - \lambda)}, \quad P = \frac{\mu\lambda\pi}{(1 + 2\chi_x\rho^2)(\lambda_0 - \lambda)l_x} \tag{42}$$

where

$$\alpha = (AD)^{1/2}, \quad \gamma = \left(\frac{A}{D}\right)^{1/2}, \quad \chi_x = \frac{\alpha}{RhG_x}$$

$$\rho = \frac{l}{\sqrt{2}l_x}, \quad l = 2\pi\left(\frac{R}{\gamma}\right)^{1/2}, \quad \lambda_0 = \frac{1}{4\rho^2} + \frac{\rho^2}{1 + 2\chi_x\rho^2}$$

and

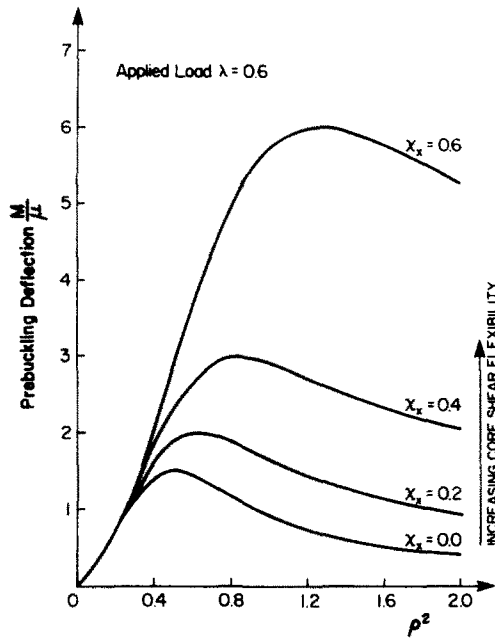


Fig. 3. Prebuckling axisymmetric lateral deflection as a function of axial shear core flexibility.

$$\lambda = \frac{N_0 R}{2\alpha}. \quad (43)$$

#### Axisymmetric buckling of a perfect cylinder

An interesting consequence of eqn (42) is that it is possible to obtain an axisymmetric buckling solution for the perfect shell at this stage of the analysis. For the case of a perfect shell,  $\mu$  vanishes and for non-zero values of  $M$ , the deflection mode as specified by eqn (41) then corresponds to the axisymmetric buckling mode of the perfect shell. The condition for non-zero values of  $M$  requires the denominator to vanish. Thus,  $\lambda = \lambda_0$  and the axisymmetric buckling coefficient ( $\lambda_a$ ) for the perfect shell is obtained by minimizing  $\lambda_0$  with respect to the axial wave number  $\rho$ . The equation  $\partial\lambda_0/\partial\rho^2 = 0$  has two real solutions, namely:

$$\rho^2 = \frac{1}{2(1-\chi_x)}, \quad \rho^2 = \infty. \quad (44)$$

When the axial core shear flexibility coefficient  $\chi_x \geq 1$ ,  $\rho^2 = \infty$  is the only real root. Substituting eqn (44) into the equation for  $\lambda_0$  yields the axisymmetric buckling coefficient  $\lambda_a$  for the perfect cylinder:

$$\begin{aligned} \lambda_a &= 1 - \frac{\chi_x}{2} \quad \text{when } \chi_x \leq 1 \\ \lambda_a &= \frac{1}{2\chi_x} \quad \text{when } \chi_x > 1. \end{aligned} \quad (45)$$

#### Growth of prebuckling lateral deflections

The amplitude of the lateral deflection  $M$  grows under increasing load. Of engineering interest is the imperfection wave number which gives the largest deflection for a given load. From eqn (42), the value of  $M$  becomes a maximum, for a given load  $\lambda$  and imperfection amplitude  $\mu$ , when  $\lambda_0$  is a minimum. As noted earlier, the axial wave number which minimizes  $\lambda_0$  is the axisymmetric buckling wave number for the perfect shell. Thus, imperfections in the shape of the classical axisymmetric buckling mode will yield the largest prebuckling deflection. Figure 3 illustrates the prebuckling deflection for various axial wave

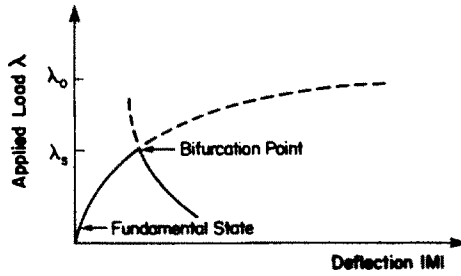


Fig. 4. Bifurcation from fundamental equilibrium path.

numbers at a given load. It is also evident that the prebuckling deflection increases with increasing axial core shear flexibility.

*Bifurcation buckling solution*

Under increasing load the amplitude of the lateral deflection  $M$  will grow in a hyperbolic fashion until the bifurcation point is reached, where there is an intersection of equilibrium paths (Fig. 4). Let us define the terms  $\bar{w}(x, y)$ ,  $f(x, y)$ ,  $b_x(x, y)$  and  $b_y(x, y)$  associated with bifurcation from the fundamental axisymmetric state. Hence, one can write,

$$F(x, y) = -\frac{1}{2}N_0y^2 + F^*(x) + f(x, y), \quad w(x, y) = w^*(x) + \bar{w}(x, y)$$

$$\beta_x(x, y) = \beta_x^*(x) + b_x(x, y), \quad \beta_y(x, y) = b_y(x, y). \tag{46}$$

The bifurcation point can be determined by considering the existence of a second solution to the governing equations which is infinitesimally close to the fundamental solution. With  $\bar{w}(x, y)$ ,  $f(x, y)$ ,  $b_x(x, y)$  and  $b_y(x, y)$  representing infinitesimal deviations from the fundamental state, after substituting eqn (46) into the governing equations [eqns (28), (29), (32)], the resulting equations can be linearized with respect to  $w(x, y)$  and  $f(x, y)$  to obtain the linearized equations of neutral equilibrium :

Compatibility equation :

$$\nabla^4 f = \frac{A}{R} \left[ \frac{\partial^2 \bar{w}}{\partial x^2} - \frac{2\gamma\rho^2\lambda_0}{(\lambda_0 - \lambda)} \mu \cos\left(\frac{2\pi x}{l_x}\right) \frac{\partial^2 \bar{w}}{\partial y^2} \right]. \tag{47}$$

Equilibrium equations :

$$b_x - \frac{\partial \bar{w}}{\partial y} = \frac{D}{G_x h} \left[ \frac{\partial^2 b_x}{\partial x^2} + \frac{(1+\nu)}{2} \frac{\partial^2 b_y}{\partial x \partial y} + \frac{(1-\nu)}{2} \frac{\partial^2 b_x}{\partial y^2} \right]$$

$$b_y - \frac{\partial \bar{w}}{\partial x} = \frac{D}{G_y h} \left[ \frac{\partial^2 b_y}{\partial y^2} + \frac{(1+\nu)}{2} \frac{\partial^2 b_x}{\partial x \partial y} + \frac{(1-\nu)}{2} \frac{\partial^2 b_y}{\partial x^2} \right]$$

$$D \left[ \frac{\partial^3 b_x}{\partial x^3} + \frac{\partial^3 b_y}{\partial x^2 \partial y} + \frac{\partial^3 b_x}{\partial x \partial y^2} + \frac{\partial^3 b_y}{\partial y^3} \right] = -\frac{2\alpha\lambda}{R} \frac{\partial^2 \bar{w}}{\partial x^2}$$

$$+ \frac{2\gamma\lambda\rho^2\mu}{(\lambda_0 - \lambda)R} \cos\left(\frac{2\pi x}{l_x}\right) \frac{\partial^2 f}{\partial y^2} - \frac{\gamma\alpha\lambda\mu}{(\lambda_0 - \lambda)R} \cos\left(\frac{2\pi x}{l_x}\right) \frac{\partial^2 \bar{w}}{\partial y^2} - \frac{1}{R} \frac{\partial^2 f}{\partial x^2}. \tag{48}$$

A rigorous solution of the above coupled equations of neutral equilibrium with given boundary conditions is extremely difficult. However, an approximate solution can be obtained using an assumed mode of the form,

$$\bar{w}(x, y) = \sum_{i=0}^{\infty} K_i \cos \frac{(2i+1)\pi x}{l_x} \cos \frac{\pi y}{l_y} \tag{49}$$

where

$$K_i = 0 \quad \text{for } i < 0.$$

Substituting the assumed mode into the compatibility [eqn (47)] and equilibrium equations [eqn (46)], exact particular solutions for  $f$ ,  $b_x$  and  $b_y$  are obtained in terms of the coefficients  $K_i$ , i.e.

$$\begin{aligned} f(x, y) &= \sum_{i=-1}^{\infty} H_i \cos \frac{(2i+1)\pi x}{l_x} \cos \frac{\pi y}{l_y}, \quad b_x = \sum_{i=0}^{\infty} A_i \sin \frac{(2i+1)\pi x}{l_x} \sin \frac{\pi y}{l_y}, \\ b_y &= \sum_{i=0}^{\infty} B_i \cos \frac{(2i+1)\pi x}{l_x} \sin \frac{\pi y}{l_y} \end{aligned} \tag{50}$$

where

$$\begin{aligned} H_i &= \frac{-2\alpha \left[ (2i+1)^2 \rho^2 K_i - \frac{\mu\gamma\rho^2\tau^2\lambda_0}{(\lambda_0-\lambda)} (K_{i-1} + K_{i+1}) \right]}{[(2i+1)^2 \rho^2 + \tau^2]^2} \\ A_i &= \frac{-K_i \left[ \frac{a_{2i}(2i+1)\pi}{l_x} - \frac{b_{1i}\pi}{l_y} \right]}{(a_{1i}a_{2i} - b_{1i}b_{2i})}, \quad B_i = \frac{-K_i \left[ \frac{a_{1i}\pi}{l_y} - \frac{b_{2i}(2i+1)\pi}{l_x} \right]}{(a_{1i}a_{2i} - b_{1i}b_{2i})} \\ a_{1i} &= 1 + \frac{\chi_x}{2} \left[ (2i+1)^2 \rho^2 + \frac{(1-\nu)}{2} \tau^2 \right], \quad a_{2i} = 1 + \frac{\chi_y}{2} \left[ \tau^2 + \frac{(1-\nu)}{2} (2i+1)^2 \rho^2 \right] \\ b_{1i} &= \chi_x \frac{(1+\nu)(2i+1)}{4} \rho\tau, \quad b_{2i} = \chi_y \frac{(1+\nu)(2i+1)}{4} \rho\tau. \end{aligned} \tag{51}$$

Since eqn (50) satisfies the first three governing equations exactly, Galerkin's procedure can then be applied to the remaining equilibrium equation to obtain an approximate solution for the buckling stress. Substituting eqn (50) into the last equilibrium equation yields the following error function :

$$\xi(x, y) = \frac{A}{(2R)^2} \sum_{i=-2}^{\infty} S_i \cos \frac{(2i+1)\pi x}{l_x} \cos \frac{\pi y}{l_y}. \tag{52}$$

In the Galerkin procedure, the error function  $\xi(x, y)$  is multiplied by

$$\cos \frac{(2j+1)\pi x}{l_x} \cdot \cos \frac{\pi y}{l_y} \quad \text{for } j = 0, 1, 2, \dots,$$

integrated over the whole shell and equated to zero. Thus,

$$\iint \xi(x, y) \cos \frac{(2j+1)\pi x}{l_x} \cos \frac{\pi y}{l_y} dx dy = 0 \tag{53}$$

yields an infinite system of linear algebraic equations for the coefficients  $K_i$  in the following form :

$$S_{-1} + S_0 = 0, \quad S_{-2} + S_1 = 0, \quad S_j = 0 \quad \text{for } j \geq 3 \tag{54}$$

where

$$\begin{aligned}
 S_i &= U_{i-1}K_{i-2} + V_iK_{i-1} + (W_i + U_{i-1} + U_{i+1})K_i + V_{i+1}K_{i+1} + U_{i+1}K_{i+2} \\
 U_i &= \frac{(2\mu\gamma\rho^2\tau^2\lambda_0)^2}{(\lambda_0 - \lambda)^2} \cdot \frac{1}{[(2j+1)^2\rho^2 + \tau^2]} \\
 V_i &= \frac{-\mu\gamma\tau^2\lambda}{(\lambda_0 - \lambda)} - \frac{4\mu\gamma\rho^2\tau^2\lambda_0}{(\lambda_0 - \lambda)} \left\{ \frac{(2i-1)^2\rho^2}{[(2i-1)^2\rho^2 + \tau^2]^2} + \frac{(2i+1)^2\rho^2}{[(2i+1)^2\rho^2 + \tau^2]^2} \right\} \\
 W_i &= k_i - 4(2i+1)^2\rho^2\chi + \frac{4(2i+1)^4\rho^4}{[(2i+1)^2\rho^2 + \tau^2]^2} \\
 k_i &= [a_{2i}(2i+1)^4\rho^4 - (b_{1i} + b_{2i})(2i+1)^3\rho^3\tau + (a_{1i} + a_{2i})(2i+1)^2\rho^2\tau^2 \\
 &\quad - (b_{1i} + b_{2i})(2i+1)\rho\tau^3 + a_{1i}\tau^4]/(a_{1i}a_{2i} - b_{1i}b_{2i}). \tag{55}
 \end{aligned}$$

ANALYTICAL RESULTS

Sandwich cylinders can be roughly classified into three categories according to their core shear flexibility:

- (a) stiff core sandwich cylinders with  $\chi_x, \chi_y < 0.1$ ;
- (b) moderately flexible core sandwich cylinders with  $0.1 \leq \chi_x$  or  $0.1 \leq \chi_y$ , and  $\chi_x, \chi_y < 0.9$ ;
- (c) weak core sandwich cylinders with  $\chi_x$  or  $\chi_y > 0.9$ .

Because of the assumption that the facings' flexural stiffness about their middle surfaces can be neglected, the results presented for weak core cylinders are not expected to be accurate.

First term approximate solution

Using only the first term

$$K_0 \cos \frac{\pi x}{l_x} \cdot \cos \frac{\pi y}{l_y}$$

in the assumed buckling mode [eqn (49)], the first equation from the set of equations [eqn (54)] is obtained. For a non-trivial solution,  $K_0 \neq 0$  gives:

$$v_0 + w_0 + u_{-1} + u_1 = 0 \tag{56}$$

or

$$\begin{aligned}
 k_0 - 4\rho^2\lambda + \frac{4\rho^4}{(\rho^2 + \tau^2)^2} - \frac{\mu\gamma\tau^2\lambda}{(\lambda_0 - \lambda)} - \frac{8\mu\gamma\rho^4\tau^2\lambda_0}{(\lambda_0 - \lambda)(\rho^2 + \tau^2)^2} \\
 + \frac{(2\mu\gamma\rho^2\tau^2\lambda_0)^2}{(\lambda_0 - \lambda)^2} \left[ \frac{1}{(\rho^2 + \tau^2)^2} + \frac{1}{(9\rho^2 + \tau^2)^2} \right] = 0. \tag{57}
 \end{aligned}$$

The above equation can be written as a cubic polynomial of  $\lambda$ :

$$\lambda^3 + P\lambda^2 + Q\lambda + R = 0 \tag{58}$$

where

$$\begin{aligned}
 P &= -(2\lambda_0 + \lambda_1 + E_1), \quad Q = \lambda_0^2 + 2\lambda_0\lambda_1 + \lambda_0 E_1 - E_2 \\
 R &= -\lambda_1\lambda_0^2 + \lambda_0 E_2 - E_3, \quad \lambda_1 = \frac{k_0}{4\rho^2} + \frac{\rho^2}{(\rho^2 + \tau^2)^2} \\
 E_1 &= \frac{\mu\lambda\tau^2}{4\rho^2}, \quad E_2 = \frac{2\mu\gamma\rho^2\tau^2\lambda_0}{(\rho^2 + \tau^2)^2}, \quad E_3 = (\mu\gamma\rho\tau^2\lambda_0)^2 \left[ \frac{1}{(\rho^2 + \tau^2)^2} + \frac{1}{(9\rho^2 + \tau^2)^2} \right]. \quad (59)
 \end{aligned}$$

### Perfect cylinders

The buckling load for a geometrically perfect sandwich cylinder can be easily obtained by setting  $\mu = 0$  in eqn (57), i.e.

$$\lambda = \frac{k_0}{4\rho^2} + \frac{\rho^2}{(\rho^2 + \tau^2)^2}. \quad (60)$$

Of particular interest is the case of axisymmetric buckling of the perfect cylinder. Thus, setting  $\tau = 0$ , the resulting expression for  $\lambda$  is minimized with respect to  $\rho$ , to give:

$$\begin{aligned}
 \lambda_a &= 1 - \frac{\chi_x}{2} \quad \text{with } \rho^2 = \frac{2}{(1 - \chi_x)} \quad \text{for } \chi_x < 1 \\
 \lambda_a &= \frac{1}{2\chi_x} \quad \text{with } \rho^2 = \infty \quad \text{for } \chi_x \geq 1. \quad (61)
 \end{aligned}$$

This of course is the same result as that obtained in eqn (45) except that  $\rho$  differs by a factor of 2 due to the difference in the definition of the buckling modes.

Because of the orthotropy of the core, the expression for  $k_0$  is complicated [see eqn (55)]. However it simplifies considerably for the case of an isotropic core and the corresponding buckling stress is,

$$\lambda = \frac{(\rho^2 + \tau^2)^2}{4\rho^2 \left[ 1 + \frac{\chi}{12}(\rho^2 + \tau^2) \right]} + \frac{\rho^2}{(\rho^2 + \tau^2)^2}. \quad (62)$$

As shown by Zahn and Kuenzi (1963), perfect sandwich cylinders with isotropic cores buckle in the axisymmetric mode and thus the buckling coefficient is given by eqn (61). In the limiting case of a non-shear deformable core eqn (62) reduces to,

$$\lambda = \frac{(\rho^2 + \tau^2)^2}{4\rho^2} + \frac{\rho^2}{(\rho^2 + \tau^2)^2}. \quad (63)$$

This is the same expression as that for an isotropic cylinder and the buckling load is obtained by minimizing  $\lambda$ . Any combination of  $\rho$  and  $\tau$  that satisfies

$$(\rho^2 + \tau^2)^2 + 2\rho^2 \quad (64)$$

will yield a minimum  $\lambda = 1$ .

As mentioned earlier, because of the complexity of the expression for the case of an orthotropic core, it is not easy to analytically minimize  $\lambda$  with respect to  $\rho$  and  $\tau$ . Consequently, numerical minimization was carried out to evaluate the "classical" buckling stress for sandwich cylinders for varying core shear flexibility coefficients  $\chi_x, \chi_y$ , as shown in Figs

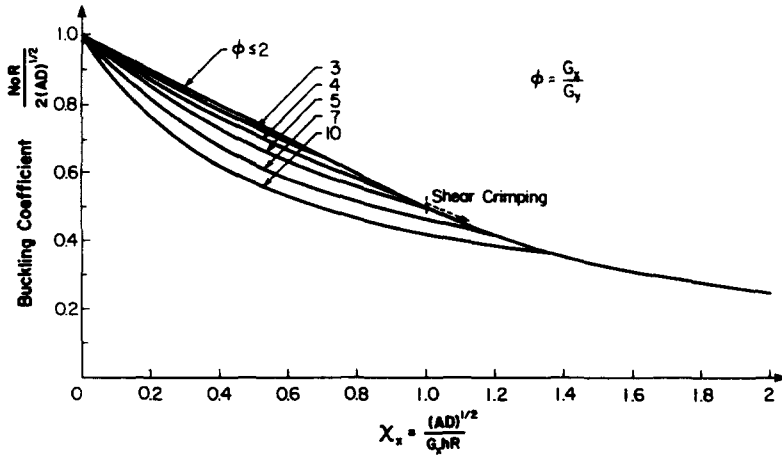


Fig. 5. Effect of orthotropic core shear stiffness ratio ( $\phi$ ) on compressive buckling strength of sandwich cylinders with isotropic facings.

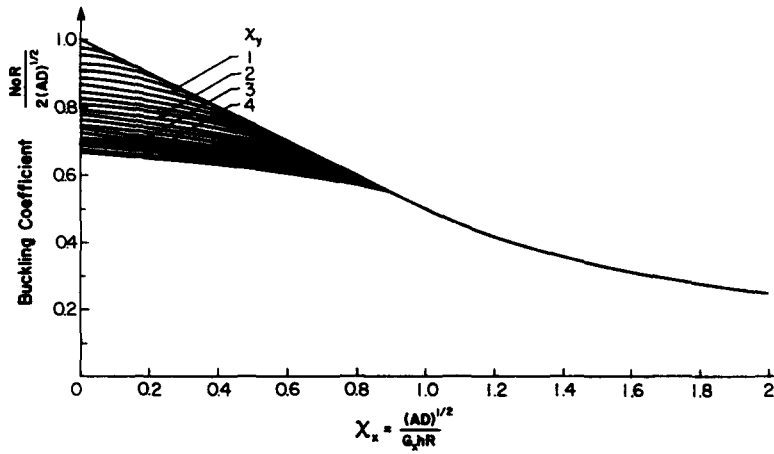


Fig. 6. Buckling coefficient for perfect sandwich cylinder with orthotropic core.

5 and 6. Results of Zahn and Kuenzi (1963) are reproduced in the case of  $\phi = 5$ , where  $\phi = \chi_y / \chi_x = G_x / G_y$ . For large values of  $\phi$  (e.g. 7, 10), the plot in Fig. 5 shows that it is possible to have a buckling load lower than the shear crimping† load (Zahn and Kuenzi, 1963) for  $\chi_x \geq 1$  in a sandwich cylinder with an orthotropic core. Numerical results indicated that for  $\phi \leq 2.0$  the sandwich cylinder buckles in the axisymmetric mode and thus the buckling coefficient is given by the simple expressions in eqn (61). For design purposes, buckling load and stress can be calculated using the following relations :

Buckling load :

$$P_c = 4\pi\alpha\lambda_c = 2\pi R N_c$$

Buckling stress :

$$\sigma_c = \frac{N_c}{(t_1 + t_2)} = \frac{E_f t_e}{R\sqrt{3(1-\nu^2)}} \tag{65}$$

where  $t_e$  = the “equivalent thickness”, which is defined as the thickness of an “equivalent” isotropic cylinder having the same ratio of in-plane to bending stiffness as the sandwich shell, i.e. from eqn (43),

† Special form of general instability having short buckle wavelength, due to low transverse shear modulus of core (Sullins *et al.*, 1969).

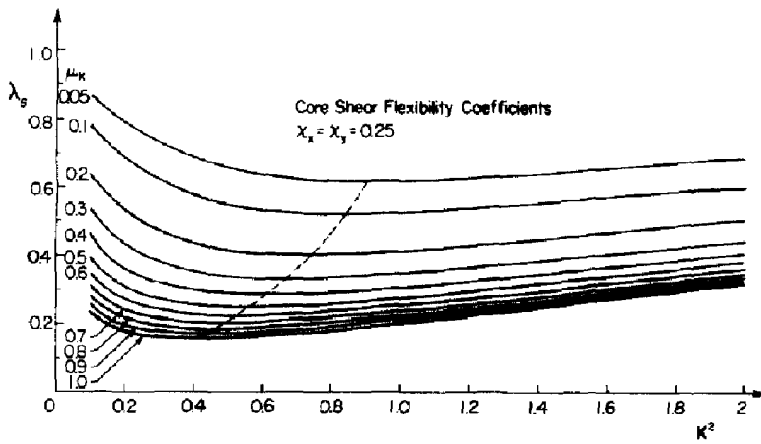


Fig. 7. Effect of imperfection amplitude on  $\lambda_s$  vs  $K^2$  for isotropic cores.

$$\gamma^2 = \left( \frac{A}{D} \right)_{isotropic} = \frac{12(1-\nu^2)}{t_c^2}$$

or

$$t_c = \frac{2\sqrt{3(1-\nu^2)}}{\gamma} \tag{66}$$

*Imperfect cylinders*

The cubic eigenvalue eqn (58) yields the bifurcation load coefficient  $\lambda_s$  for an axisymmetric imperfect sandwich cylinder by minimizing  $\lambda$  with respect to the circumferential wave number  $\tau$  for a given imperfection wave number  $\rho$ . Because of the complexity of the equation, the minimization is done numerically and the smallest real root of the cubic eigenvalue equation is selected.

For the case of a non-shear deformable core ( $\chi_x = \chi_y = 0$ ), the cubic eigenvalue equation reduces to that for an isotropic cylinder when the nondimensional imperfection parameter is taken in the form  $\mu_k = \mu/t_c$ . Thus the analytical results for isotropic shells can be applied to "stiff-core" sandwich cylinders.

The next class of cylinders considered is that for isotropic cores ( $\chi_x = \chi_y$ ). Figures 7, 8 and 9 are plots of the bifurcation load coefficient  $\lambda_s$  versus imperfection amplitude ( $\mu_k$ ) and the wave number parameter  $K^2 = \rho^2/\rho_c^2$  where  $\rho_c^2 = 1/[2(1-\chi_x)]$  is the classical axisymmetric buckling mode wave number. It can be seen that there exists a critical axial wave number where the degradation is largest for a given imperfection amplitude. The dashed

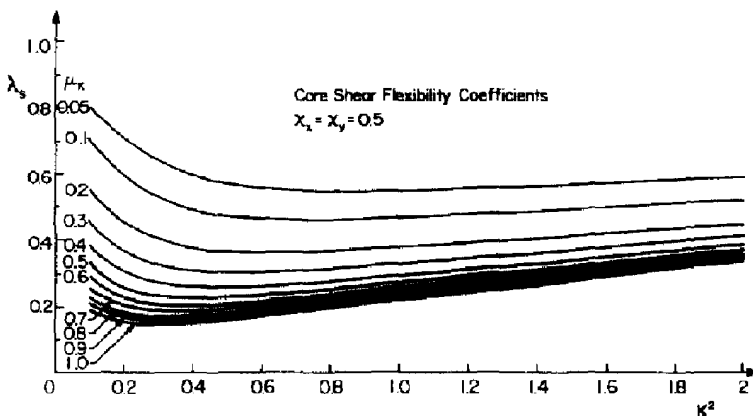


Fig. 8. Effect of imperfection amplitude  $\mu_k$  on  $\lambda_s$  vs  $K^2$  for isotropic cores.



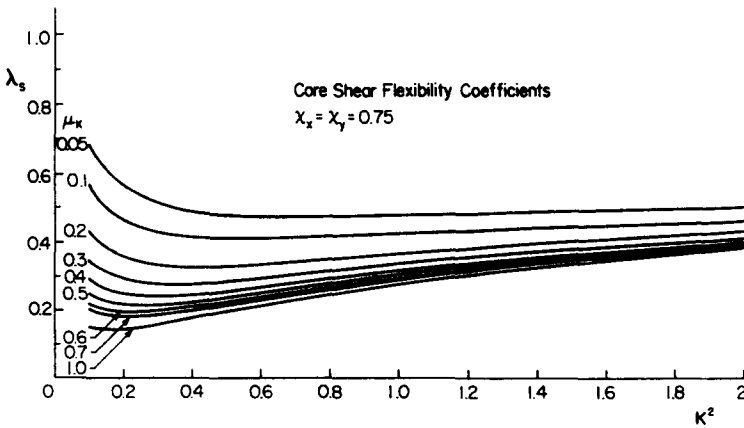


Fig. 9. Effect of imperfection amplitude  $\mu_\kappa$  on  $\lambda_s$  vs  $K^2$  for isotropic cores.

line in Fig. 7 joins the critical wave number for each imperfection amplitude. The critical wave number decreases with increasing imperfection. From these three figures it can also be seen that critical  $K^2$  decreases with increasing core shear flexibility. Figure 10 demonstrates that imperfections can lead to buckling loads below the shear crimping value of the "perfect" cylinder, although these results maybe somewhat inaccurate for  $\chi_x > 0.9$ .

For the case of orthotropic cores, it is apparent from Fig. 12 that the circumferential core shear flexibility coefficient  $\chi_y$  has little effect on the critical buckling mode wave number

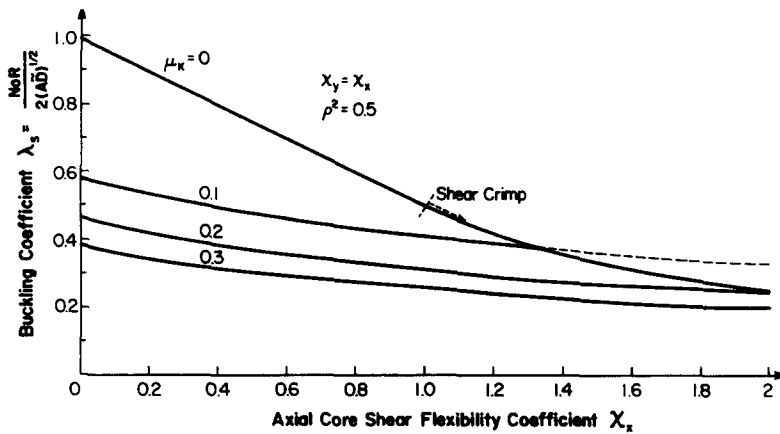


Fig. 10. Effect of imperfection amplitude on  $\lambda_s$  vs  $\chi_x$  for isotropic cores.

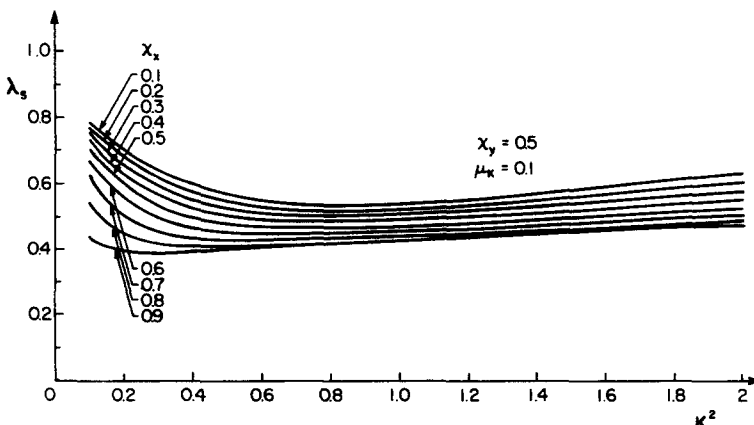


Fig. 11. Effect of  $\chi_x$  on imperfect orthotropic honeycomb sandwich cylinders.

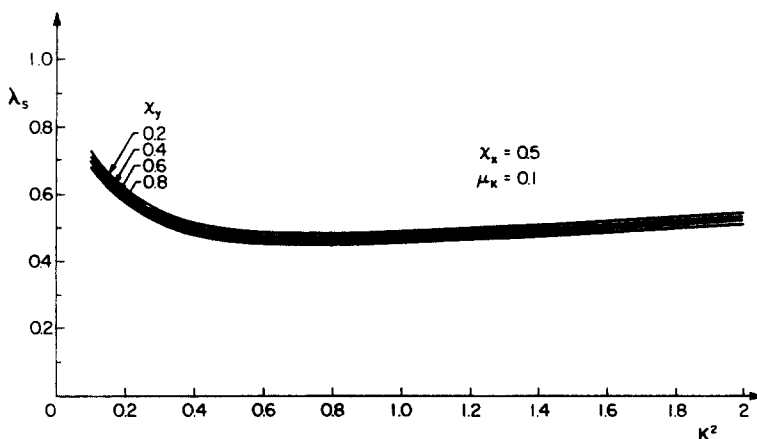


Fig. 12. Effect of  $\chi_y$  on imperfect orthotropic honeycomb sandwich cylinders.

( $K^2$ ). However, Fig. 11 reveals that the critical  $K^2$  parameter decreases with increasing axial core shear flexibility. In general it can be noted that increasing core shear flexibility  $\chi_x, \chi_y$  decreases the buckling strength.

From an engineering design viewpoint, it is useful to plot a “knock-down” factor corresponding to the minimum buckling load ( $\lambda_m$ ) associated with the critical wave number, as a function of the non-dimensional imperfection parameter  $\mu_k$ . Figures 13 and 14 present

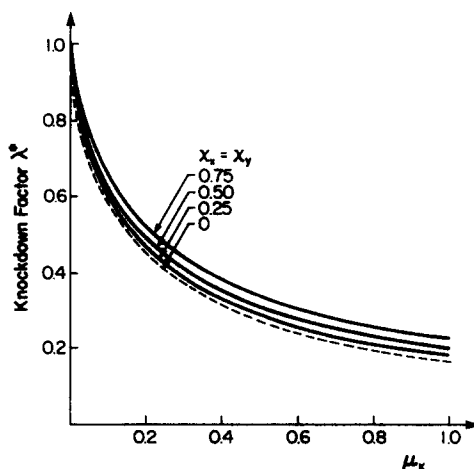


Fig. 13. Effect of core shear flexibility coefficient on  $\lambda^*$  vs  $\mu_k$  for isotropic core.

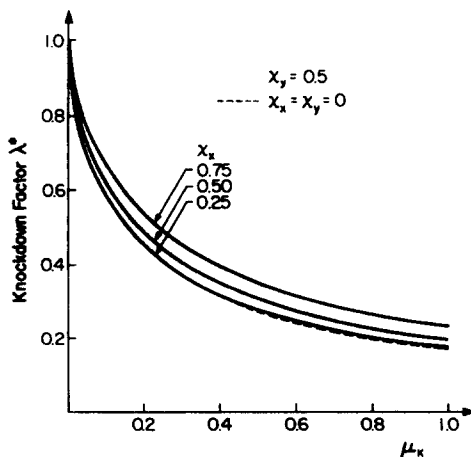


Fig. 14. Effect of axial core shear flexibility ( $\chi_x$ ) on  $\lambda^*$  vs  $\mu_k$  for orthotropic core.

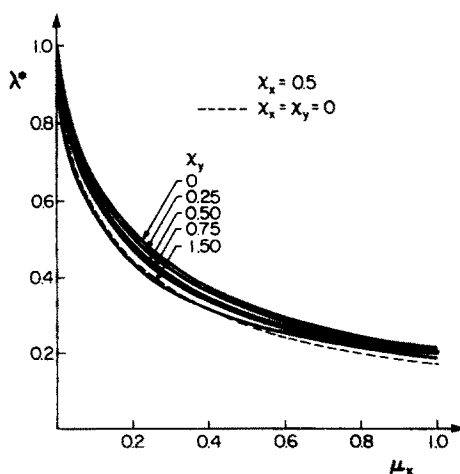


Fig. 15. Effect of axisymmetric shape imperfections and circumferential core shear flexibility ( $\chi_y$ ) on compressive buckling strength for orthotropic cores.

such plots for isotropic and orthotropic cores, respectively. The “knock-down” factor is defined as  $\lambda^* = \lambda_m/\lambda_c$ , where  $\lambda_c$  is the perfect cylinder buckling coefficient, as determined from eqn (60). Again it is evident that decreasing the core flexibility coefficients decreases  $\lambda^*$ . However, it is interesting to note from Fig. 15, that for a fixed value of  $\chi_x = 0.5$ , increasing the circumferential core flexibility coefficient  $\chi_y$  actually decreases  $\lambda^*$ . In each of these three graphs, the non-shear deformable core case is shown, which corresponds to the isotropic cylinder solution as discussed earlier. In most instances, it provides a lower bound curve for the solutions obtained.

### CONCLUSIONS

Solutions have been obtained for axisymmetric imperfect sandwich cylinders having isotropic facings and orthotropic shear deformable cores. Shear core flexibility has been shown to have a significant effect on the buckling strength, both for the perfect and imperfect cylinders. For very stiff cores, buckling behaviour is very similar to that of an isotropic shell based on an “equivalent” thickness formulation. Finally, it is worth noting that the “knock-down” curves presented can be used to assist the design engineer in calculating the load reductions for sandwich cylinders containing random imperfections following the methodology described in Tennyson *et al.* (1971) providing an estimate of the maximum root mean square imperfection amplitude is known.

*Acknowledgement*—The authors wish to gratefully acknowledge the financial support of our shell mechanics program by the Natural Sciences and Engineering Research Council of Canada under Grant A-2783.

### REFERENCES

- Almroth, B. O. (1964). Buckling of axially compressed sandwich cylinders. TR 6-62-64-9, Lockheed Missiles and Space Co., Sunnyvale, CA, July 1964.
- Barteld, G. and Mayers, J. (1967). Unified theory for the bending and buckling of sandwich shells—application to axially compressed circular cylindrical shells. AIAA/ASME 8th Structures, Structural Dynamics and Materials Conf., Palm Springs, CA 29–31 March 1967.
- Cheung, E. W. and Tennyson, R. C. (1988). Buckling of composite sandwich cylinders under axial compression. In Studies in Applied Mechanics 19. *Buckling of Structures—Theory and Experiment*, The J. Singer Anniversary Volume (Edited by I. Elishakoff, J. Arbocz, C. D. Babcock and A. Libai), Elsevier, Amsterdam.
- Leggett, D. M. A. and Hopkins, H. G. (1949). Sandwich panels and cylinders under compressive end loads. British Aeronautical Research Council Reports and Memoranda, No. 2262.
- March, H. W. and Kuenzi, E. W. (1957). Buckling of cylinders of sandwich construction in axial compression. Report 1830, Forest Products Laboratory, Madison, WI, June 1952, rev. December 1957.
- Plantema, F. J. (1966). *Sandwich Construction*. Wiley, New York.
- Reese, C. D. and Bert, C. W. (1969). Simplified design equations for buckling of axially compressed sandwich cylinders with orthotropic facings and core. *AIAA J. Aircraft* 6(6), November–December 1969.

- Reese, C. D. and Bert, C. W. (1974). Buckling of orthotropic sandwich cylinders under axial compression and bending. *AIAA J. Aircraft* **11**(4), April 1974.
- Stein, M. and Meyers, J. (1952). Compressive buckling of simply supported curved plates and cylinders of sandwich construction. NACA TN 2601, January 1952.
- Sullins, R. T., Smith, G. W. and Spier, E. E. (1969). Manual for structural stability analysis of sandwich plates and shells. NASA CR-1457, December 1969.
- Teichmann, F. K., Wang, Chi-Teh and Gerard G. (1951). Buckling of sandwich cylinders under axial compression. *J. Aeronaut. Sci.* June 1951.
- Tennyson, R. C., Muggerridge, D. B. and Caswell, R. D. (1971). New design criteria for predicting buckling of cylindrical shells under axial compression. *AIAA J. Spacecraft Rockets* **8**(10).
- Wang, C. T., Vaccaro, R. J. and Desant, D. F. (1955). Buckling of sandwich cylinders under combined compression, torsion, and bending load. *J. Appl. Mech.* **22**(3), September 1955.
- Zahn, J. J. and Kuenzi, E. W. (1963) Classical buckling of cylinders of sandwich construction in axial compression—orthotropic cores. U.S. Forest Service Note, FPL-018, November 1963.